

Boletim de Ciências Geodésicas

ISSN: 1413-4853 ISSN: 1982-2170

Universidade Federal do Paraná

Ferreira, Luiz Danilo Damasceno; Moraes, Rodolpho Vilhena de A procedure for assessing the thermal reemission effects on CBERS 04A Boletim de Ciências Geodésicas, vol. 28, no. 2, e2022008, 2022 Universidade Federal do Paraná

DOI: https://doi.org/10.14482/INDES.30.1.303.661

Available in: https://www.redalyc.org/articulo.oa?id=393972085001



Complete issue

More information about this article

Journal's webpage in redalyc.org



Scientific Information System Redalyc

Network of Scientific Journals from Latin America and the Caribbean, Spain and Portugal

Project academic non-profit, developed under the open access initiative

ORIGINAL ARTICLE

A procedure for assessing the thermal reemission effects on CBERS 04A

Luiz Danilo Damasceno Ferreira¹ ORCID: 0000-0002-8247-313X Rodolpho Vilhena de Moraes² ORCID: 0000-0003-1289-8332

¹Universidade Federal do Paraná, Programa de Pós Graduação em Ciências Geodésicas, Curitiba, Paraná, Brasil. E-mail: luizdaniloferreira@gmail.com

²Universidade Federal de São Paulo, Instituto de Ciência e Tecnologia, São José dos Campos, São Paulo, Brasil. E-mail: rodolpho.vilhena@gmail.com

Received in 08th July 2021. Accepted in 15th May 2022.

Abstract:

Thermal reemission affects satellite orbits when a recoil force results from the emission of radiation from the satellite surface. In this study, the analysis of the thermal reemission force on the satellite is made separately, that is, when the satellite (CBERS 04A's main body and the solar panels) are hit by the sunlight and when the satellite is into the shadow. Thus, it is presented an expression in an exponential form in order to explain the behavior of the perturbation due to thermal reemission on the panels when they are inside the Earth's shadow. Both the time spent into the shadow and the relaxation time of the solar panels allowed an analysis of the behavior of the disturbing acceleration and of the orbital elements, during cooling and heating processes. The results presented in this study are promising in terms of practical applications.

Keywords: CBERS 04A; Thermal reemission force; Relaxation time; Thermal reemission effects.

How to cite this article: FERREIRA, L.D.D. and MORAES, R.V. A procedure for assessing the thermal reemission effects on CBERS 04A. *Bulletin of Geodetic Sciences*. 28(2): e2022008, 2022.



1. Introduction

Most Earth Resource Satellites orbits are at a height of about 750 km and the main disturbance acting on their orbits are caused mainly by the non-uniform distribution of the Earth's mass, the gravitational attractions of Moon and the Sun, the pressure of solar radiation, the atmospheric drag and the indirect gravitational effects of the Sun and the Moon. But there are others small non-gravitational forces such as, among others, the Earth's albedo, electromagnetic perturbations, Lense-Thierring effect, Poynting-Robertson effect, Yarkovsky-Schach effect, and thermal reemission force that cannot be neglected in order to obtain an accurate orbit for such satellites. This work deals with the disturbance due to the thermal reemission force, also taking into account the passage of the satellite through the Earth's shadow. An application is done considering the CBERS 04A satellite.

Thermal reemission effect is due to the solar heating and affects satellite orbits when a recoil force results from the emission of radiation from the satellite surface. This force is known as thermal reemission force, it depends on a satellite's effective cross-sectional area and of the orientation of the satellite in space, i.e., its attitude. The modeling of the thermal reemission on satellites presents a reasonable degree of complexity due to the irregular shape of the satellite. In this study, smaller structures (e.g. antennas) contribute to the effective area, but their shapes are not considered (Rodriguez-Solano et al. 2012)

The CBERS 04A (China-Brazil Earth Resources Satellite), shown in Figure 1 is a three-axis-stabilized satellite with complex shape and different absorption and reflection features for each component at its surface. The CBERS 04A orbit is about 630 km. For this satellite, the axes are right-handed system with the origin at the satellite center of mass (cm). The Z_s axis is pointed to nadir (Earth's surface). The Y_s axis is parallel to the solar panels and the X_s axis completes the right-handed system, as shown in Figure 2.



Source: https://cbers04A.inpe.br

Figure 1: CBERS 04A

The aim of this research is to present the disturbance due to the thermal reemission force on the CBERS 04A, taking into account the model developed by Afonso et al. (1989). These authors present a model for the thermal reemission force when the satellite is under the shadow of the Earth. Due to this fact, in this paper the analysis of the thermal reemission force on the satellite (CBERS 04A's main body and the solar panels) is made separately, that is, when the satellite is hit by the sunlight and when the satellite is into the shadow.

Nowadays the satellites are covered in Multi-Layer Insulation (MLI) which is composed by multiple layers of thin sheets. MLI blankets are the most common insulation, though single layer barriers are sometimes used where lesser degrees of insulation are required because they are lighter and less expensive (Boushon 2018).

The thermal reemission forces on CBERS 04A's main body and on the solar panels are estimated because the satellite complexity is not considered.

2. Thermal reemission forces

The CBERS 04A's main body is assumed to have a box shape and almost all its faces are covered with 15-layered MLI blankets, except the parts with radiators which are painted in S781 white paint for the faces with less solar incidence (Costa and Wang 2015). The MLI contributes with a large part of the thermal reemission force. The Optical Solar Reflector (OSR) areas are not considered. Thus, this force can be expressed as (Zierbart et al. 2003; Adhya 2005; Duha et al. 2006)

$$d\vec{F}_{b} = -\frac{2}{3} \frac{\varepsilon \sigma T_{A}^{4}}{c} dA\vec{n} \tag{1}$$

where ϵ is the emissivity, σ is the Stephan-Boltzmann constant, T_A is the temperature of the element of area dA, c is the speed of the light and \vec{n} the unit vector normal to the emitting surface. Integrating Equation 1 over the body surface, the thermal reemission force is

$$\vec{F}_b = -\frac{2}{3} \frac{\varepsilon_{mli} \sigma A_b T_s^4}{c} \vec{n}$$
 (2)

where A_b is the mean cross-section area-body, ϵ_{mli} is the emissivity of the MLI and T_s the temperature of the satellite's body, which is assumed to be uniformly distributed.

CBERS 04A solar panels consist of many thin layers of materials sandwiched together to form a composite structure. According to Costa et al. (2015), the panels with large heat dissipation equipment, where additional heat transfer capability was needed, had aluminum-ammonia axially grooved Heat Pipes installed both embedded into honeycomb panels and in the extern surface.

The solar panels are treated as planar surfaces remaining always Sun-facing, and their temperatures are modeled as a function of Sun-panels distance and taking into account the material properties of each layer in the panels. The thermal reemission force on the panels can be evaluate by integrating Equation 1 over the solar panels (Zierbart et al. 2003; Adhya 2005; Duha et al. 2006)

$$\vec{F}_{p} = -\frac{2A}{3} \frac{(\varepsilon_{f} T_{f}^{4} - \varepsilon_{b} T_{b}^{4})}{c} \vec{n}$$
(3)

where A is the panels area, T_f and T_b , ε_f and ε_b are the temperatures and the emissivity of the front and back solar panels, respectively, and the unit vector normal to the panels.

Dividing Equation 2 by the CBERS 04A's mass M_c and Equation 3 by the solar panel's mass M_p , the total thermal reemission acceleration, when the satellite is hit by the sunlight, is given by (Duha et al. 2006)

$$\vec{A}_{bp} = \left[-\frac{2A_b}{3M_c} \frac{\epsilon_{mli} \sigma T_s^4}{c} - \frac{2A}{3M_p} \frac{(\epsilon_f T_f^4 - \epsilon_b T_b^4)}{c} \right] (\sin\phi \vec{x}_s + \cos\phi \vec{z}_s)$$
(4)

 ϕ , is the angle between the satellite–Sun vector \vec{S} and the unit vector \vec{z}_s , \vec{x}_s , \vec{y}_s , \vec{z}_s are the unit vectors in the CBERS 04A-fixed reference system, as shown in Figure 2.

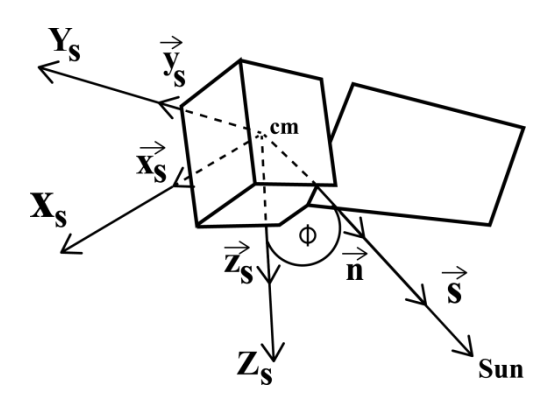


Figure 2: Unit vectors \vec{x}_s , \vec{y}_s , \vec{z}_s .

Table 1 and Table 2 present the material properties and the temperatures used in the box shape MLI model and in the solar panels, respectively. The material properties values have been difficult to find in this analysis since data on the properties of these surfaces were not available and are assumed to remain constant throughout the satellite's orbit. The material parameters influence the thermal reemission force which are calculated and have effect on the satellite trajectory. The temperatures are approximated and remain constant in the orbits.

Table 1: CBERS 04A's body material properties and temperature.

Parameter	Value
$oldsymbol{arepsilon}_{mli}$	0.7
T_s	314.1 K
σ	5.6699 x 10 ⁻⁸ W/m ² K ⁴

Source: R.L. Costa, personal communication, 2021.

Table 2: Solar panels material properties and temperature.

Parameter	Value
$\epsilon_{_{\mathrm{f}}}$	0.87
$\epsilon_{_{ m b}}$	0.88
T _f	327.1 K
T_{b}	324.3 k

Source: R.L. Costa, personal communication, 2021.

3. Thermal reemission forces into the Earth's shadow

Morescki (2006) presents an exponential expression modeling the behavior of the perturbation due to thermal reemission on the panels into the Earth's shadow, which is based on the model proposed by Afonso et al. (1989). The panels continue to emit the thermal reemission in a short time after entering shadow (cooling process) and takes a short period of time to reach the same thermal configuration (heating process) as before entering shadow. A simple cylindrical shadow model is used, and it is sufficient to determine whether the satellite is in Earth' shadow or not (Cappelari et al. 1976).

Thus, the expression of the thermal reemission force on the panels can be expressed by equation below

$$\vec{F}_{ps} = \begin{cases} -|\vec{F}_{p}|e^{\frac{-(t-t_{1})}{\tau_{p}}} & t_{1} \leq t \leq t_{2} \\ -|\vec{F}_{p}|C_{p}\left[1 - e^{\frac{-(t-t_{2})}{\tau_{p}}}\right] + |\vec{F}_{p}|e^{\frac{-t_{e}}{\tau_{p}}} & t_{1} \leq t \leq t_{2} + \tau_{p} \end{cases}$$
(5)

where C_n is given by the following equation

$$C_{\rm p} = \frac{1 - e^{\frac{-t_{\rm e}}{\tau_{\rm p}}}}{1 - \frac{1}{\rho}} \tag{6}$$

 t_1 is the shadow entry time, t is the time counted from the right ascension node, t_2 is the time of exiting from shadow, t_e is the time spent in shadow, $t_1 \le t \le t_2$ is the cooling process, $t_1 \le t \le t_2 + \tau_p$ is the heating process, $(t - t_1)$ is the time measured since the satellite entry into shadow, $(t - t_2)$ is the time measured since the satellite left the shadow, τ_p is the relaxation time of the temperature gradient and e is the base of natural logarithms.

Relaxation time is when the solar panels reach thermic equilibrium after entering shadow and can be obtained by the approximate solution of the heat conduction equation in one dimension. Because the thickness of the solar panels is much smaller compared to the other dimensions, one can consider the heat flow in the direction from the front face to the back face of the solar panels. Thus, the equation of relaxation time is

$$\tau_{\rm p} = \frac{\rho C_{\rm s}}{\pi^2 K_{\rm t}} d^2 \tag{7}$$

where, ρ is the density (Kg/m³), C_s specific heat (J/Kg K), K_t is the thermal conductivity (W/m K) of solar panels layers, d is the thickness (mm) and its numerical values are defined in Table 3.

Material	Thickness (mm)	Specific Heat (J/Kg K)	Thermal Conductivity (W/m K)	Density (Kg/m³)
Coverglass	0.120	720	1.506	3121
Adhesive 1	0.02	1040	0.146	1080
Solar Cells	0.20	720	150.000	2651
Adhesive 2	0.08	1040	0.310	1510
Kapton Foil	0.05	1040	0.155	1420
Adhesive 2	0.08	1040	0.310	1510
Carbon Fiber	0.1	840	1.300	1650
Al. Honeycomb	21.0	963	0.776	16
Carbon Fiber	0.1	840	1.300	1650

Table 3: Characteristics of solar panels layers.

Source: R.L. Costa, personal communication, 2021.

Dividing Equation 5 by the solar panel's mass M_p , the total thermal reemission acceleration due to solar panels, is given by (Duha et al. 2006).

$$\vec{A}_{ps} = \begin{cases} -\left| \frac{\vec{F}_{p}}{M_{p}} \right| e^{\frac{-(t-t_{1})}{\tau_{p}}} & t_{1} \leq t \leq t_{2} \\ -\left| \frac{\vec{F}_{p}}{M_{p}} \right| C_{p} \left[1 - e^{\frac{-(t-t_{2})}{\tau_{p}}} \right] + \left| \vec{F}_{p} \right| e^{\frac{-t_{e}}{\tau_{p}}} & t_{2} \leq t \leq t_{2} + \tau_{p} \end{cases}$$
(8)

4. Equations of motion

The quantitative prediction of the perturbation on the CBERS 04A is made in two steps:

a) The equation of motion is assumed to include the two body gravitational effect (reference orbit)

$$\ddot{\vec{r}} = -\frac{GM}{r^3}\vec{r} \tag{9}$$

b) Including only thermal reemission acceleration disturbance (perturbed orbit)

$$\ddot{\vec{r}} = -\frac{GM}{r^3}\vec{r} + \vec{A} \tag{10}$$

the vector \vec{A} is composed of two parts (\vec{A}_{bp} and \vec{A}_{bs}) corresponding to Equation 4 and Equation 8, respectively, GM is the geocentric gravitational constant of the Earth, \vec{r} is the geocentric position vector, $r = |\vec{r}|$. The difference between the reference and perturbed orbits deviations gives the effects of the perturbation in time. Both Equation 9 and Equation 10 are solved numerically using the Runge-Kutta method of seventh-eighth-order (Fehlberg 1968), with the same initial conditions. The solutions of these equations furnish the positions vectors \vec{r} and the velocities vectors \vec{v} , expressed on Cartesian Inertial System (CIS). Transformations were performed to get the corresponding orbital elements at any instant of time (Bate et al. 1971, pp.61).

The thermal reemission perturbations deviations, from the differences between reference orbit and perturbed orbit, can be better visualized in the RNT coordinate system with the origin at the satellite center of mass. In this system, the radial component R is defined in the direction and sense of the satellite geocentric radius vector, the normal component N is perpendicular to the orbital plane and the component along track T is perpendicular to R and N and is also along the velocity vector (Seeber 2003, pp.87; Heilmann et al. 2013). The equations of the deviations produced on RNT components are presented in Appendix A. This perturbation on the orbital elements can be visualized by the differences between reference orbital elements and perturbed orbital elements. The equations of these differences are also showed in Appendix B.

5. Results and discussions

The initial conditions required to solve numerically Equation 9 and Equation 10 is given in Table 4. The orbital elements are obtained from TLE (NASA/NORAD (2020) (Two-Line Element at 12^h 06^m 02^s UTC January 11^{th} 2021) and transformed in state vector (\vec{r}, \vec{v}) . The step-size (Δt) used was 10 seconds, the total propagation time of these equations was 7680 seconds (128 minutes) and one assumes that temperatures of the satellite's body and solar panels do not change throughout the satellite's orbit.

Semi-major axis	а	7002675.072 m
Eccentricity	е	0.0001596
Inclination	i	97.9413
Right ascension node	Ω	91.6557
Argument of perigee	ω	85.2103
Mean anomaly	М	274.9287
M_{b}		1925 kg
$M_{\mathtt{p}}$		55 kg
A		16.38 m²
A_{b}		4.5 m ²
GM		3.986008 m³/s²

Source: the authors.

The value of τ_p is on the order of 1 second which leads solar panels to reach thermal equilibrium as soon as they enter into Earth's shadow and returns instantly the former thermal configuration when it leaves the shadow. The Relaxation time was determined by Equation 7 with the values defined in Table 3.

The variations of the RNT components of the position are shown in Figure 3. On the axis of time, the reference epoch is 12^h 06^m 02^s UTC January 11^{th} 2021 and the time interval is 10 seconds. The transverse component is the most affected one, where the deviation amounts to 0.032 m in 128 minutes, while the radial component deviates around -0.00097 m and the normal component deviates around -0.0058 m.

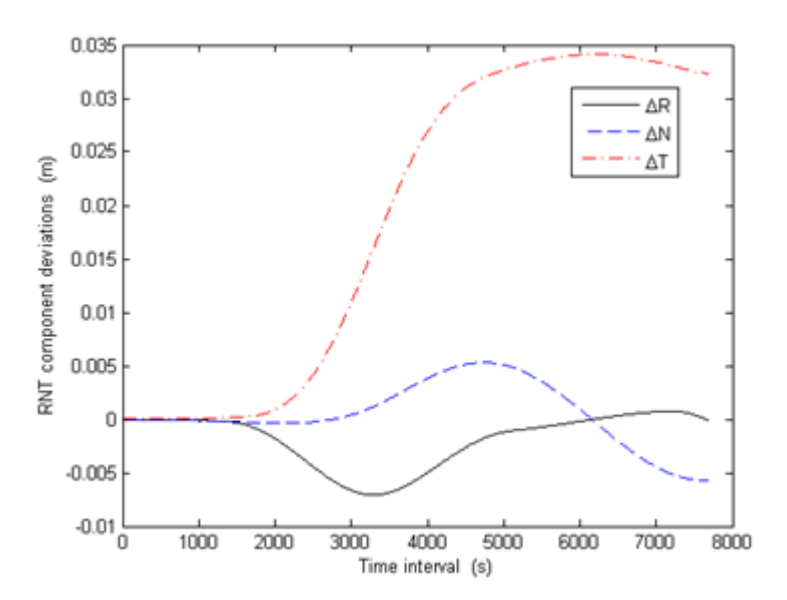


Figure 3: RNT components of the position RNT.

In Figure 4 it is shown the amplitude variations of the thermal reemission acceleration components A_x , A_y and A_z , respectively. Concerning the amplitude of the accelerations when satellite is in sunlight period the components of the thermal acceleration can have positives and negatives amplitude, with values on the order of 10^{-9} m/s². When the satellite is under the shadow period (approximately 34 minutes), during the cooling and the heating processes, the values of the components decline on the order of 10^{-13} m/s². This fact is due to thermal equilibrium and it means that in shadow, the period that the thermal reemission force has effect on the satellite trajectory. The magnitude of

the perturbation acceleration is in the range of A = $6.858 \times 10^{-9} \text{ m/s}^2$ when the satellite is in sunlight and A = 1.083×10^{-13} m/s² when it is under the shadow, according to Figure 5.

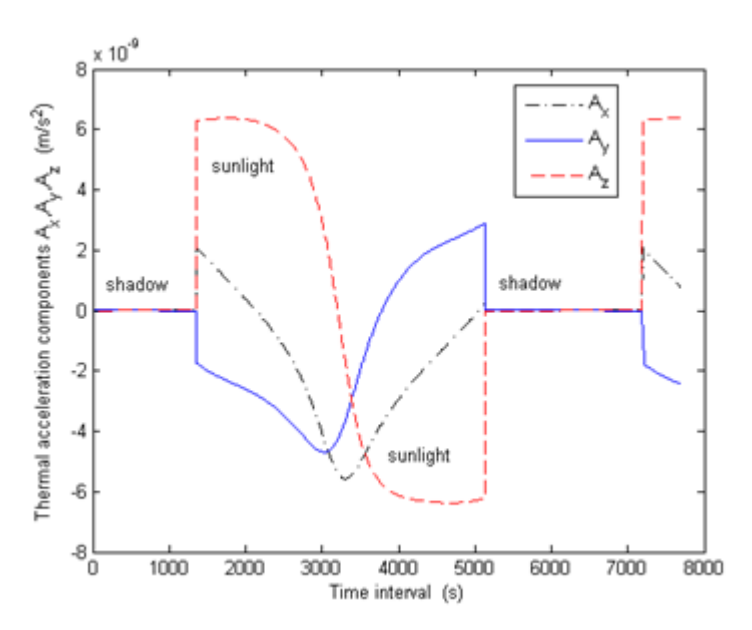


Figure 4: Thermal reemission acceleration components A_x, A_y A_y.

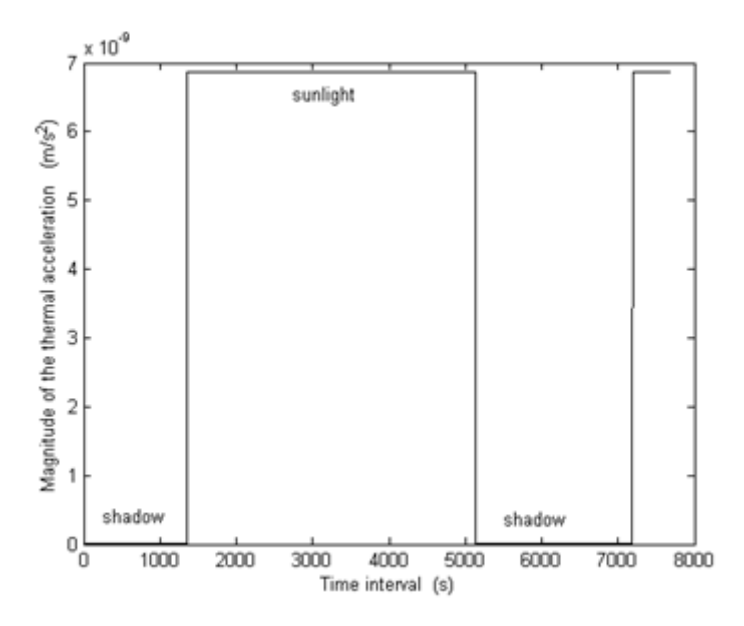


Figure 5: Magnitude of the thermal acceleration A.

In Figure 6 it is showed the differences of semi-major axis (Δa) due to the thermal perturbation effect and can be seen that such effect produces a small oscillation around 4.8×10^{-3} m when the satellite is in sunlight. When the satellite enters into shadow, the value is around -2.7×10^{-4} m, then it drops to -6.19×10^{-7} m and after exiting the shadow the value is around -0.00026 m. The changes of these values are due to thermal equilibrium of the solar panels.

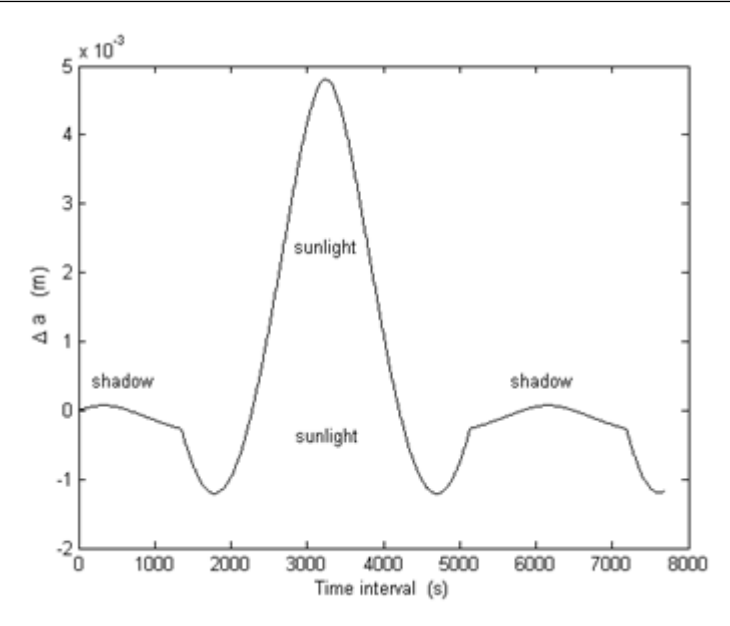


Figure 6: Variation of semi-major axis Δa .

Figure 7 shows that the differences Δe , Δi and $\Delta \Omega$ are not affected by the thermal reemission force and in Figure 8 it is possible to observe that $\Delta \omega$ and ΔM are affected by a small oscillation with maximum amplitude on the order of 10^{-4} degrees when the satellite is in sunlight and 10^{-5} degrees when the satellite is in the shadow.

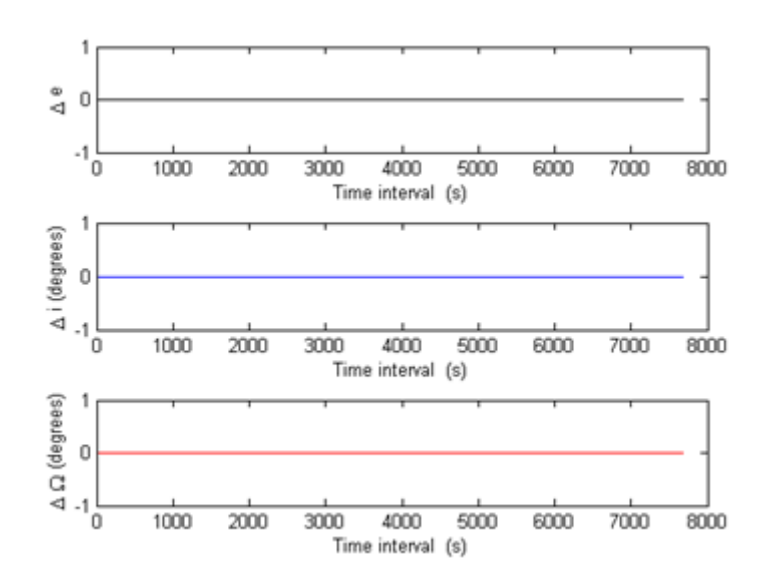


Figure 7: Variations of Δ e, Δ i and Δ Ω.

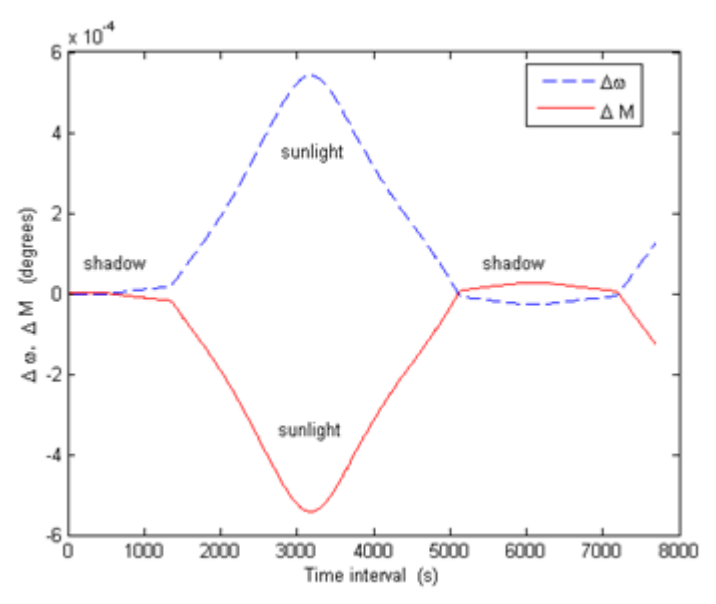


Figure 8: Variations of $\Delta \omega$ and ΔM .

6. Final considerations

In this study, the equation of motion for CBERS-04A are assumed to include the two body gravitational effect (reference orbit) and thermal reemission force only (perturbed orbit) and the effect of this last disturbance on the satellite can be observed by comparing the reference orbit with the perturbed orbit along the time.

The results presented can be extended for other type of satellite, modifying the following hypotheses considered here: the main body of satellites as a box, the solar panels as planar surfaces and an exponential model for the thermal reemission forces on the panels when they are into the Earth's shadow.

The thermal reemission force causes variations the orbital elements (a, ω , M) and these effects can be evaluated during the orbit propagation.

Both the time spent into the shadow and the relaxation time of the solar panels allowed an analysis of the behavior of the disturbing acceleration and of the orbital elements above mentioned, during cooling and heating processes.

The orbital deviations due to RNT components and mainly the deviation of semi-major axis are small but cannot be neglected in the modeling for precise orbit determination of the CBERS 04A satellite.

Also, the small, but uninterrupted alteration of the semi-major axis caused by thermal reemission, over time, cause the satellite to reach denser layers of the atmosphere, contributing to an increase of the drag action and, consequently, the duration that the satellite should continue to work in orbit.

AUTHOR'S CONTRIBUTION

All authors contributed equally.

REFERENCES

ADHYA, S. Thermal Re-radiation Modelling for the Precise Prediction and the Determination of Spacecraft Orbits. London, Thesis (Doctor of Philosophy), Department of Geomatic Engineering, University College London, 2005.

AFONSO, G. B., BARLIER, F., CARPINO, M., FARINELLA, P., MIGNARD, F., MILANI, A. &NOBILI, A.M. Orbital effects of LAGEOS seasons and eclipses. *Annalae Geophysicae*, v. 7: 501-514, 1989.

BATE, R.R., MUELLER, D.D., WHITE, J.E., Fundamentals of Astrodynamics. New York, N.Y., 1971, 455p.

BOUSHON, K. E. *Thermal analysis and control of small satellites in low Earth orbit*. Master of Science in Aerospace Engineering, Missouri University of Science and Technology, 2018.

CAPPELARI, J., VELEZ, C., FUCHS, A. *Mathematical Theory of the Goddard Trajectory Determination System*. **GSFC** Document X-582-76-77, Greenbelt, 1976.

CBERS 04A. Available at: https://cbers04A.inpe.br [Accessed 09 November 2021].

COSTA, R. L.; WANG, T; VLASSOV, V; LIYIN, G. *CBERS-4 Satellite Thermal Design and Flight Model Environmental Thermal Tests*. 45th International Conference on Environmental Systems ICES-2015-28 12, Bellevue, Washington, 16 July 2015

DUHA, J., AFONSO, G.B., FERREIRA, L.D.D. Thermal reemission effects on GPS satellites. *J. Geodesy,* **80,** 665–674, https://doi.org/10.1007/s00190-006-0060-x , 2006.

FEHLBERG, E. Classical Fifth-, Sixth-, Seventh-, And Eighth-Order Runge-Kutta Formulas with Step size Control. Washington. D.C., NASA (NASA TR R-287), 1968.

HEILMANN, A., FERREIRA, L.D.D., DARTORA, C.A., NOBREGA, K.Z. Antenna radiation effects on the orbits GPS and INTELSAT satellites. *Acta Astronautica*, v.88, p. 1-7, 2013.

MORESCKI, Jr. *Modelagem da força de re-emissão* **térmica sobre o** *satélite GPS durante sua passagem pela sombra da Terra*. Curitiba, Dissertação (Mestrado em Ciências Geodésicas) Setor de Ciências da Terra, Universidade Federal do Paraná, 2006.

NATIONAL AERONAUTICS AND SPACE ADMINISTRATION (NASA/NORAD). National Space Science Data Center – Definition of two-line element set coordinate system. 2011.

SEEBER, Günter. Satellite Geodesy. 2. Ed. Berlin: Walter de Gruyter, 2003. 589p.

RODRIGUEZ-SOLANO., HUGENTOBLER, U., STEINGENBERGER, P. Adjustable box-wing model radiation pressure impacting GPS satellites. *Advances in Space Research*, v.49, p. 1113-1128, 2012.

ZIEBART, M., ADYA, S., SIBTHORPE, A., CROSS, P., "GPS Block IIR Non-Conservative Force Modeling: Computation and Implications," *Proceedings of the 16th International Technical Meeting of the Satellite Division of The Institute of Navigation (ION GPS/GNSS 2003)*, Portland, OR, September, p. 2671-2678, 2003.

Appendix A - RNT deviations

In this Appendix, the equations of RNT deviations are presented.

$$\Delta R = \frac{1}{r_r} [(x_r - x_p)x_r + (y_r - y_p)y_r + (z_r - z_p)z_r]$$
 (A1)

$$\Delta N = \frac{1}{G} [(x_r - x_p)G_x + (y_r - y_p)G_y + (z_r - z_p)G_z]$$
 (A2)

$$\Delta T = \frac{1}{r_r G} [(x_r - x_p) H_x + (y_r - y_p) H_y + (z_r - z_p) H_z]$$
 (A3)

$$\begin{split} r_{r} &= (x_{r}^{2} + y_{r}^{2} + z_{r}^{2})^{\frac{1}{2}} \\ &\vec{G} = \vec{r}_{r} \times \vec{v}_{r} \\ G &= \left(G_{x}^{2} + G_{y}^{2} + G_{z}^{2}\right)^{\frac{1}{2}} \\ G_{x} &= y_{r}v_{rz} - z_{r}v_{ry} \\ G_{y} &= z_{r}v_{rx} - x_{r}v_{rz} \\ G_{z} &= x_{r}v_{ry} - y_{r}v_{rx} \\ &\vec{H} &= \vec{r}_{r} \times \vec{G} \\ H_{x} &= \frac{1}{r_{r}G} \left(z_{r}G_{y} - y_{r}G_{z}\right) \\ H_{y} &= \frac{1}{r_{r}G} \left(x_{r}G_{z} - z_{r}G_{x}\right) \\ H_{z} &= \frac{1}{r_{r}G} \left(y_{r}G_{x} - x_{r}G_{y}\right) \end{split}$$

 $\mathbf{r_r} = |\vec{\mathbf{r}}_r|$, is the modulus of the geocentric position vector of the satellite at the reference orbit.

 x_r , y_r , z_r , are the components of \vec{r}_r ;

 $v_r = |\vec{v}_r|$, is the modulus of the velocity vector of the satellite at the reference orbit;

 v_{rx} , v_{ry} , v_{ry} , are the components of \vec{v}_r ;

 $r_p = |\vec{r}_p|$, is the modulus of the geocentric position vector of the satellite at the perturbed orbit;

 x_{n} , y_{n} , z_{n} , are the components of \vec{r}_{n} ;

 \vec{G} , is the momentum angular;

 G_{x} , G_{y} , G_{z} , are the components of \overrightarrow{G} ;

 H_{\downarrow} , H_{\downarrow} , are the components of \overrightarrow{H} .

Appendix B - Orbital elements differences

In this Appendix, the equations of orbital elements differences are presented.

$$\Delta a = a_{\rm r} - a_{\rm p} \tag{B1}$$

$$\Delta e = e_r - e_p \tag{B2}$$

$$\Delta i = i_r - i_p \tag{B3}$$

$$\Delta\Omega = \Omega_{\rm r} - \Omega_{\rm p} \tag{B4}$$

$$\Delta\omega = \omega_r - \omega_p \tag{B5}$$

$$\Delta M = M_r - M_p \tag{B6}$$

a_r, e_r, i_r, Ω_r , ω_r , M_r, are the orbital elements of the satellite at the reference orbit;

 $\mathbf{a_{_p},\,e_{_p},\,i_{_p},\,\Omega_{_p},\,\omega_{_p},\,M_{_p},\,are\,\,the\,\,orbital\,\,elements\,\,of\,\,the\,\,satellite\,\,at\,\,the\,\,perturbed\,\,orbit.}$